CONTEMP. PHYS., 1978, VOL. 19, NO. 4, 289–310

Structure Determination by X-ray Absorption

E. A. STERN
University of Washington, Seattle, Washington 98195, U.S.A.

ABSTRACT. The present article describes the basic physics and some applications of a new technique for structure determination using X-ray absorption. The extended X-ray absorption fine structure (EXAFS) on the high energy side of absorption edges contains structure information on the local atomic environment surrounding the absorbing atom. Because EXAFS supplies the local structure about each type of atom in the sample, separately, without requiring crystallinity of the sample, it makes feasible structure measurements in many systems which have defied previous analysis by standard techniques. Some examples of diverse applications of the technique are given such as: characterizing adsorbed surface atoms; studying catalysts; measuring the environment around the metal atom in metalloproteins; determining the structure of liquids, glasses and amorphous solids; and measuring solids under high pressure. The article concludes by pointing out how the intense X-ray sources recently produced by synchrotron radiation have made EXAFS measurements simpler and speedier.

1. Introduction

Traditionally, the absorption and emission of electromagnetic radiation has been a very powerful probe of the electronic energy states of matter. In fact, the basic concept of the discrete character of the energy levels of atoms was ascertained by this means. On the other hand, the diffraction of electromagnetic radiation in the X-ray region is a very important tool for determining the atomic arrangement of matter. This separation between the role of absorption and emission on one hand and diffraction on the other has been recently bridged by the realization that the absorption of X-ray radiation is also a powerful tool to determine the arrangement of atoms.

The absorption of X-rays by atoms is smoothly varying with photon energy except at some discrete energies where abrupt increases occur called absorption edges. These edges correspond to the X-ray photon attaining enough energy to excite additional occupied electron levels in the atom. The absorption of X-rays on the high energy side of absorption edges does not vary monotonically in condensed matter but has a complicated behaviour which extends past the edge by an amount typically of the order of 1 keV, as illustrated in fig. 1 for the K-edge of copper metal. This non-monotonic variation has received the name of extended X-ray absorption fine structure (EXAFS) and it only occurs when atoms are present in condensed matter. Isolated atoms do not show this fine structure so that clearly EXAFS is caused by the presence of surrounding atoms.

As we will discuss, it is possible to invert these data and obtain the location of the first few nearest neighbour atoms surrounding the absorbing atom. The EXAFS has been known for over 40 years but only recently has this power for structure determination been appreciated (Sayer, Stern and Lytle 1971). This paper will focus on the recent developments. The status of X-ray absorption before the recent developments is given in the review of Azaroff and Pease (1974).

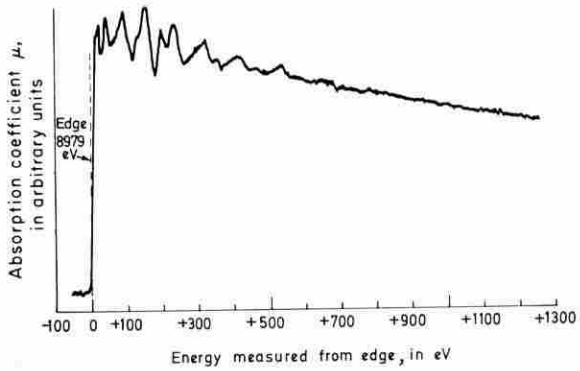

Fig. 1. The K-edge of copper metal showing the extended X-ray absorption fine structure. The energy of the X-ray photon is shown on the horizontal scale measured from the edge. The K-edge energy is 8979 eV.

The technique is so useful because it opens the possibility of making studies which are not possible by diffraction techniques. The characteristics of structure determination by EXAFS are:

(*a*) The local atomic environment around each kind of atom in a sample is determined by EXAFS. By tuning the X-rays to the absorption-edge energy of an atom, only its environment is probed. Since EXAFS measures only short range order, there is no fundamental distinction between crystals with long range order and samples without, such as amorphous solids, liquids, and solutions. Thus aperiodic systems can be studied with the same ease as crystals.

(*b*) In principle, the kinds of surrounding atoms can be distinguished by the energy dependence of their contribution to the EXAFS.

(*c*) The number of atoms at a given average distance and the disorder in their location about the average can be quantified by EXAFS.

(*d*) In unoriented samples only the radial distance between the centre atom and its neighbouring atoms is determined, but in oriented samples which have less than cubic symmetry, angular positions are discernible.

(*e*) Determination of the chemical state of the atom is possible by determining absorption edge shift and the near-edge structure.

The basic experimental arrangement is particularly simple. As illustrated in fig. 2 the monochromatic incident X-ray beam has a fixed fraction of its intensity I_0 sampled by detector (1) while another detector (2) measures the intensity I that passes through the sample. Generally, it is found that

$$I = I_0 \exp(-\mu x) \tag{1}$$

where μ is the X-ray absorption coefficient and x is the sample thickness. The EXAFS is defined as the normalized oscillatory part of μ and is given by

$$\chi = (\mu - \mu_0)/\mu_0 \tag{2}$$

where μ_0 is the smoothly varying portion of μ past the edge and physically corresponds to the absorption coefficient of an isolated atom.

In order to understand the analysis of EXAFS for determining the positions of surrounding atoms we must understand the basic mechanism of the effect. We first of all describe this basic mechanism.

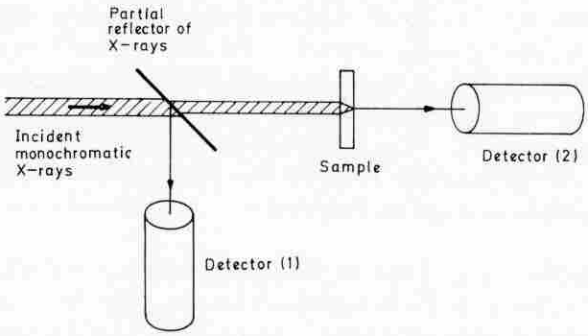

Fig. 2. Illustrating the elements needed to measure X-ray absorption. Detector (1) monitors the incoming intensity I_0 while detector (2) monitors the intensity I transmitted through the sample.

2. The basic EXAFS mechanism

The attenuation of X-rays passing through matter occurs by three principal means: scattering, photoelectric absorption, and pair production. In the X-ray regime where EXAFS occurs the photoelectric absorption dominates the attenuation process. This is fortunate because EXAFS is a product of only the photoelectric process.

Photoelectric absorption is the complete absorption of a photon which, in turn, gives its full energy to electrons. The most important case for EXAFS is when only a single electron is excited, so we start with this. The process can be calculated semiclassically treating the photon as a classical electromagnetic (EM) field and treating the electron quantum mechanically. The wavelength of the EM field is always large compared to the dimensions of the core state that is excited and thus the field can be treated as uniform in its overlap with the core state. This approximation is usually referred to as the dipole approximation. The absorption of the EM field is treated to first order in the field and thus can be calculated from the ' Golden Rule '. In these approximations the absorption coefficient μ of a sample of N_0 atoms of one kind per unit volume is given by:

$$\mu = 4N_0\pi^2e^2(\omega/c)|<\mathrm{f}|z|\mathrm{i}>|^2\rho(E_\mathrm{f}) \tag{3}$$

Here $|\mathrm{i}>$ is the initial core state, $>|\mathrm{f}$ is the final state of the photoelectron, ω is the radial frequency of the X-ray photon whose energy is $\hbar\omega$, $\rho\ (E_\mathrm{f})$ is the density of final states, and c is the velocity of light. Since the EM field can be treated as uniform in space, it can be approximated by a scalar potential which is proportional to the distance z when the X-ray polarization is in the z-direction as assumed here. By conservation of energy $\hbar\omega = E_\mathrm{fi}$, the difference in energy between the final and initial states.

2.1. *Qualitative description*

The oscillatory contribution to μ can come from only the matrix element and/or $\rho\ (E_f)$ in eqn. (3). For X-ray energies sufficiently above the edge $\rho\ (E_f)$ gives a monotonic contribution because it can be closely approximated by the free electron value. In fact, it is this characteristic that makes EXAFS so useful. The EXAFS extends to sufficiently high energies above the edge that the photoelectron can be closely approximated as a free electron and any corrections are small and easily treated. For this reason it is useful to divide the fine structure into two regimes: one, EXAFS extending from about 50 eV on upward above the edge; and two, the near edge structure consisting of all the structure below 50 eV. The near edge structure is much more difficult to calculate since the interaction between the photoelectron and the sample is strong and no simple approximations suffice. In this section we consider only the EXAFS.

The only possible contribution to EXAFS remaining is the matrix element. The variation in the matrix element itself occurs only from variation in $|f>$ since $|i>$ is fixed at a given core level. The variation in $|f>$ can be understood in a simple manner as illustrated in fig. 3. When an atom is in the condensed state so that it is surrounded by other atoms within dimensions of the order of ångströms, its photoelectron state $|f>$ is a sum of outgoing and scattered portions. If the atom were isolated its photoelectron would consist of only an outgoing wave to describe the electron escaping from the atom. Such a state contributes only a smooth absorption as measured experimentally and expected theoretically. The oscillatory behaviour occurs because of the addition of the backscattered waves from the surrounding atoms which interfere with the outgoing part. This interference will either decrease or increase the photoelectron wave function in the region of the initial state $|i>$ (that is, near the origin) depending on whether this interference is destructive or constructive. The phase between the outgoing and incoming parts can be varied by varying the photon energy which, in turn, varies the electron wavelength. The change in the photoelectron's wave function amplitude correspondingly modifies the overlap with the core state in the dipole matrix element and the absorption. Thus, the EXAFS is a direct consequence of the wave nature of the photoelectron and the peaks correspond to constructive interference between the

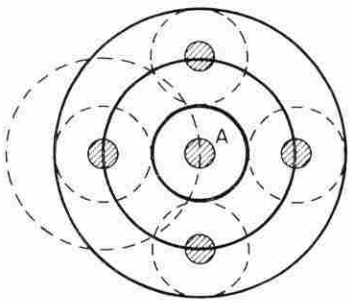

Fig. 3. Representing the composition of the final-state photoelectron $|f>$. The shaded circles represent atoms, and the full circles the photoelectron created by absorption of an X-ray photon by the atom A. The broken circles represent the further contribution due to scattering from neighbouring atoms.

outgoing and scattered parts at the origin while the valleys correspond to destructive interference. The X-ray absorption monitors the interference of the $|f>$ photoelectron state with itself.

2.2. *The basic formula*

The basic formula used to describe EXAFS is obtained by directly transcribing the above qualitative picture into a mathematical form. The result is for an unoriented sample (Stern, 1974; Stern, Sayers and Lytle, 1975)

$$\chi(k)=\frac{m_e}{4\pi\hbar^2 k}\sum_j \frac{N_j}{R_j^2}t_j(2k)\exp(-2R_j/\lambda_e)\exp(-2\sigma_j^2k^2)\sin 2[kR_j+\delta_j(k)] \quad (4)$$

An electron of momentum p has, by the de Broglie relation, associated with its wavefunction a wave number k and wavelength λ given by $k=2\pi/\lambda=p/\hbar$. The argument of the sine gives the phase difference between the outgoing and backscattered portions of the photoelectron wave function. Besides the usual term $2kR_j$, which counts the phase shift as a free electron of wave number k traverses the distance $2R_j$, additional phase shifts $\delta_j(k)$ are introduced by the fact that the electron is in the presence of potentials. The phase shift δ_j has two contributions, one from the centre atom and the other from the backscattering atom since the scattering amplitude is, in general, complex. The magnitude of the backscattering amplitude is denoted by $t_j(2k)$ and is a function of the type of atom and of k. The strength of the contribution to EXAFS from neighbours the same average distance R_j away (which we call a shell of *atoms*) will be proportional to the number N_j of such atoms of type j in that shell. The factor R_j^2 reflects the product of the amplitudes of the outgoing and backscattered waves, both of which drop off as R_j^{-1}, because of their spherical nature. The Debye-Waller type factor $\exp(-2k^2\sigma^2)$ takes account of the phase mismatch of the backscattering from the shell of atoms which have an r.m.s. disorder σ about their average shell distance of R_j. This disorder may be thermally induced and/or structural in origin. To take account of the finite lifetime of the excited state consisting of the photoelectron and the ionized atom the phenomenological term $\exp(-2R_j/\lambda_e)$ is added in the expectation that such effects can be approximated by a mean free path λ_e (which is equivalent to assuming an exponential decay in time of the excited state). The rest of the factors are not qualitatively important but enter when the detailed calculation is performed.

It is useful to emphasize that the physical simplicity of EXAFS, as exemplified by eqn. (4), comes about because multiple scattering effects are usually negligible. It is sufficient to treat the scattering from each of the surrounding atoms just once before interfering at the origin and not worry about the scattered waves bouncing off other atoms in between, before returning to the origin. In this simplification, EXAFS contrasts with another electron probe technique, low energy electron diffraction (LEED), where multiple scattering effects are generally important. The interpretation of LEED measurements, when one wants to discover anything more than unit cell dimensions, is difficult, requiring detailed and extensive model calculations. As we shall see EXAFS is much more straightforward to interpret.

2.2.1. *Distinguishing neighbouring atoms*

The k-dependence of the backscattering amplitude in eqn. (4) has been measured in various cases. This amplitude has also been calculated by Lee and Beni (1977) as a function of atomic number, Z, revealing a systematic variation consistent with experimental results. Fig. 4 illustrates the general trend. As the atomic number of the scatterer increases, the peak in $t(2k)$ moves to higher values of k, its magnitude decreases, and the backscattering persists to higher k-value. It is informative to compare the behaviour of $t(2k)$ with that of the atomic scattering factor of X-rays, $f(k)$. For X-rays $f(k)$ is equal to the Fourier transform of the electron charge density in the atom. Since all atoms have approximately the same size the k-dependence of $f(k)$ is approximately the same. Only its magnitude changes in proportional to the total electronic charge in the atom. The scattering of X-rays is then proportional to the atomic number Z of an atom and in a solid with a mixture of light and heavy atoms the scattering would be dominated by the heavy atoms.

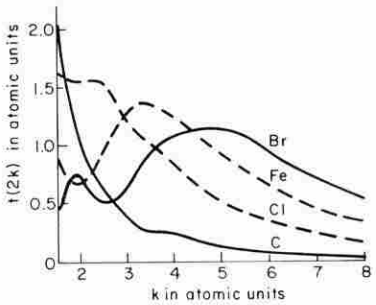

Fig. 4. The dependence of the backward scattering amplitude $t(2k)$ on k for various types of atom. The atomic unit is the reciprocal of the Bohr radius. Such a variation can be used to identify the backscattering atom.

For EXAFS the magnitude of the peak in $t(2k)$ does not change drastically with Z so that the effect is not dominated by any one class of atoms in a mixture. Thus, the contributions of light atoms are not smothered by those of heavy atoms. Equally important, the significant variation in the k-dependence of $t(2k)$ permits a distinction to be made between atoms in different rows in the periodic table.

The k-dependence of the envelope of $\chi(k)$ also has a contribution from the Debye-Waller factor $\exp(-2k^2\sigma^2)$ in eqn. (4). Since the k-dependence of $t(2k)$ is a means of identifying neighbouring atoms it is necessary to separate out the contribution of the Debye-Waller factor. This can be done at times by changing temperature and thus the thermal vibration contribution to σ^2.

The oscillatory contribution to $\chi(k)$ comes from the sine term in eqn. (4) which contains information on the distance to the neighbouring shells of atoms, R_j. If $\delta_j(k)$ were not present, the frequency of oscillation with respect to k would be a direct measure of R_j. However, the k-dependence of $\delta_j(k)$ also contributes to the frequency, e.g., if $\delta_j(k)$ can be expanded in powers of k so that $\delta_j(k)=\delta_0+\delta_1 k$, then the frequency in k is proportional to $R_j+\delta_1$. Thus the phase $\delta_j(k)$ contributes a shift to the position of atoms and this shift must be

determined in some manner in order to obtain R_j. The phase shift $\delta_j(k)$ has contributions δ_e and δ_b from both the emitting and backscattering atoms, respectively. These contributions have been calculated for the K-edge EXAFS by Lee and Beni (1977). Their results are illustrated in fig. 5 for representative atoms; $\delta_j(k)$ is obtained by simply adding the appropriate pairs of phase shifts. Again there is a Z dependence which may be a useful guide to distinguishing the scattering atom.

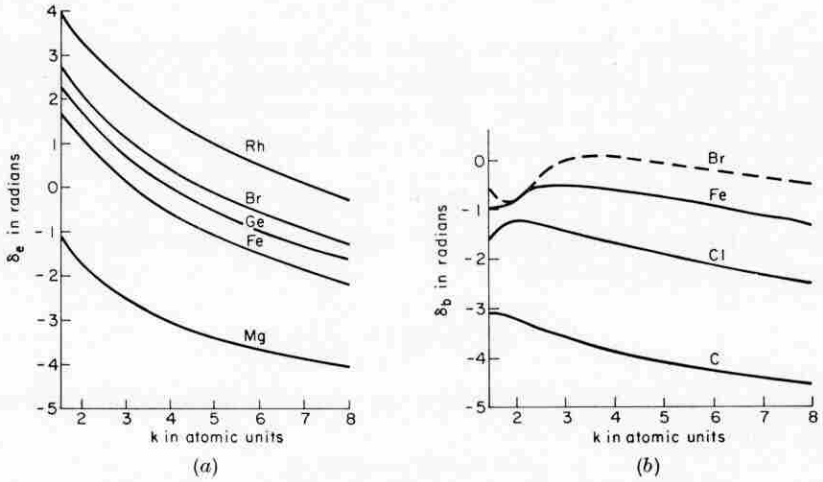

Fig. 5. The dependence on k, for various types of atom of the phase shifts (*a*) $\delta_e(k)$ due to the emitting atom and (*b*) $\delta_b(k)$ due to the backscattering atom.

2.2.2. *Transferability*

A basic assumption in employing EXAFS for quantitative structure determination is that $\delta_j(k)$ and $t(2k)$ are both independent of the chemical environment. Such an independence when the change in chemical environment is small was found experimentally in the early development years of EXAFS as a tool for investigating structure. A later study indicated that for the systems studied $\delta_j(k)$ was invariant under large chemical changes in the environment for the particular cases studied. There are, however, other experimental indications that both $\delta_j(k)$ and $t(2k)$ change when the chemical environment is varied very considerably. In some extreme cases a large change in $t(2k)$ may occur. This question still remains to be clarified by further study. Some further discussion of this is presented in Section 2.5. However, in cases where the unknown is compared with a standard with similar chemical environment, changes in $\delta_j(k)$ and $t(2k)$ do not introduce important errors in structure determinations. This point will be further illustrated in Section 6.

2.3. *Anisotropy*

The expression for EXAFS given in eqn. (4) assumed that the sample had no particular orientation. If the sample were anisotropic in this respect the EXAFS could also be anisotropic permitting some angular dependence in the structure to be ascertained. The theory of anisotropy in EXAFS can be

derived on a macroscopic basis by relating X-ray absorption to Maxwell's equations. A general electromagnetic plane wave, of wave number q and radial frequency ω, propagating in the x-direction can be represented as

$$E = E_0 \exp(iqx) \tag{5}$$

where E_0 is the amplitude of the wave. Maxwell's equations give that

$$q^2 = \frac{n^2\omega^2}{c^2}$$

where the refractive index n is related to the relative permittivity of the medium ϵ_r (usually a complex number) at the frequency ω by $\epsilon_r = n^2$ and c is the speed of light in a vacuum. We assume that the magnetic permeability of the medium is that of a vacuum. In the X-ray region

$$\epsilon_r = 1 + i\epsilon_2$$

where ϵ_2 is real and much less than 1. Substituting this value of $\epsilon_r = n^2$ into the expression for q^2 one finds

$$q = (\omega/c)\left(1 + \frac{i\epsilon_2}{2}\right)$$

Substituting this expression for q into eqn. (5) and taking the absolute square of both sides gives

$$I = I_0 \exp(-\omega\epsilon_2 x/c) \tag{6}$$

Comparing eqn. (6) and eqn. (1) leads to the relation for the X-ray absorption coefficient

$$\mu = \frac{\omega\epsilon_2}{c} \tag{7}$$

Since ϵ_2 is a tensor of rank two, μ also is a tensor of rank two in the X-ray range. The orientation-dependence of ϵ_2 (that is, the variation of ϵ_2 with the angle between the polarization vector of the electromagnetic wave and the sample axes) is well known. If a rotation axis has three-fold or higher symmetry, ϵ_2, and thus μ, is independent of this angle and thus remains constant during rotation.

2.4. *The L-edge*

The L-edge and other lower energy edges can be expected also to show EXAFS effects. The L-edge has been studied in detail and shown to be as useful for structure determination as the K-edge.

2.5. *Many-body effects*

The physics employed up to now to describe the EXAFS process is in the framework of the independent particle model where each electron is acted upon by an external potential whose value is independent of the motion of the other electrons. In reality, electrons interact with one another through the Coulomb potential and this interaction does depend on the states of the other electrons and so cannot be entirely accounted for by the independent particle model. Solid state physics is blessed by the circumstance that this many-body

effect is negligible in most cases. Is EXAFS as favoured? This question has not been fully resolved in all cases but certainly for most cases investigated to date the independent-particle description serves for analysing EXAFS and determining structure, to a satisfactory degree of accuracy.

However, there are some theoretical and experimental reasons to suspect that a full understanding of EXAFS may require accounting for many-body effects. Even the independent model eqn. (4) has some many-body effects incorporated into it. The mean free path λ has contributions from electron–electron scattering.

There are other many-body effects not accounted for at all in eqn. (4). The most obvious is that the atomic electrons in the excited atom see a different potential after a core electron has been knocked out. For the outer atomic electrons this new potential is closely approximated by that of the atom with its Z increased by 1. This different potential is one consequence of the Coulomb repulsion between electrons since its share of the shielding of the positive nucleus by the core electron is removed as the atom is excited, by removing that electron, increasing the attraction of the nucleus for the other electrons, ' pulling in ' the wave functions of the original atom, and thus relaxing them to a lower energy.

The electrons whose wave functions are relaxed are called ' passive ' electrons because they are not directly excited by the X-ray, in contrast to the core electron, the so-called ' active ' electron. However, these passive electrons still affect the absorption of the X-ray. The matrix element of eqn. (3) should, in the exact treatment, include for the initial state the full wave function of the all of the electrons in the unexcited atom, and for the final state the wave function of the excited atom and the photoelectron. In the independent particle model the wave function of the atom is simply a product of wave functions for each electron. If relaxation is neglected the passive electron states would not change as the atom is excited and their contribution to the matrix element consists of simply the product of their overlaps before and after excitation, i.e.

$$\prod_i |<p_i|p_i>|^2 = 1$$

where $|p_i>$ is the wave function of the ith passive electron. Thus, in this case the passive electrons give a factor of one and the expression in eqn. (3) need only contain the active electron states. However, if the ith passive electron state relaxes to $|p'_i>$ in the excited atoms, then the contribution of the passive electrons becomes

$$\prod_i |<p_i'|p_i>|^2 < 1.$$

This product is less than one because $|p_i'>$ is normalized and its overlap with $|p_i>$ can only be as great as one if it is equal to $|p_i>$. Thus the many-body relaxation effect reduces the value of μ below that given by eqn. (3). Estimates of this factor range between 0·6 and 0·9 in typical cases.

There is a sum rule for the dipole matrix elements in eqn. (3) which states that the total absorption integrated over all energies must be the same regardless of many-body effects. Thus, the reduction factor cannot be the only many-body effect, and it is not. The reduction in the single electron

excitation due to the reduced overlap is compensated for by multi-electron excitations. Although the X-ray photon interacts directly with only the active electron, this active electron can excite other electrons through their Coulomb interaction. Such a process is described by a different expression than eqn. (3).

The important aspect of the multi-electron excitations is that they tend not to produce EXAFS. Consider a two electron excitation into the continuum. Conservation of energy in this case requires that the sum of the energies of the two electrons be constant, but the energy of each electron can vary from zero up to the maximum possible energy. The EXAFS from this process will have contributions from electrons with varying energies and values of k, which tends to smear out the oscillations. Thus, one expects the main contribution to be the single electron excitation calculated by eqn. (3) whose contribution should be subject to the reduction factor.

If this reduction in EXAFS were a constant independent of the chemical environment, it could be normalized out by measuring a standard and would not be a problem. Unfortunately, there is both theoretical and experimental evidence that, in some cases, the variation with chemical environment is significant. However, if the chemical environments are similar the variations of the parameters in EXAFS are also small.

The lesson to be drawn is that determination of $\delta(k)$ and $t(2k)$ should be made on systems which are as chemically similar to that of the unknown as possible.

3. Interpretation

The previous discussion has (one hopes) been convincing that structure information is given by EXAFS and is given in a direct fashion. One of its strengths is that this information is easily accessible without need for complicated calculations or modelling. The simplest method to determine structure from EXAFS is to Fourier transform with respect to the wave number k. Referring to eqn. (4) we note that since the k-dependence of the other terms vary slowly as compared to the sine function, a Fourier transform of $k\chi(k)$ with respect to $\exp[-\mathrm{i}2(kr+\delta_j(k))]$ will peak around the value of $r=R_j$ locating the neighbouring shells of atoms. This is illustrated in fig. 6 which shows the Fourier transform of the copper data of fig. 1. Since EXAFS retains all phase information of the interference of the photoelectron wave function between its outgoing and backscattered waves, the Fourier transform displays all information available from the system. There is no phase problem as in X-ray diffraction which measures the intensity of the diffracted wave and not its amplitude, losing information about the phase of the diffracted wave. In the case of X-ray diffraction, modelling the atomic structure of the sample, calculating the diffraction pattern of the model, and varying the model to obtain a best fit with the measured pattern can give additional information on the structure beyond that obtainable simply from Fourier transforming, in contrast to EXAFS.

There are two types of Fourier transforms employed presently. One uses theoretical values of $\delta_j(k)$ in the Fourier transform to obtain R_j directly. The other type is to transform with respect to $\exp(-\mathrm{i}2kr)$ without including $\delta_j(k)$ in the transform. In this case, as discussed in the previous Section, the peak

occurs at $R_j + \delta_1$ where δ_1 is an appropriate average of the first derivative of $\delta_j(k)$ with respect to k. To correct for the effects of $\delta_j(k)$ on the transform requires a calibration which is usually done by measuring the EXAFS on a standard whose structure is known and which approximates the chemical environment of the unknown as much as possible. An advantage of the second transform over the first is its minimization of any chemical effects that may be present, as discussed in the previous Section.

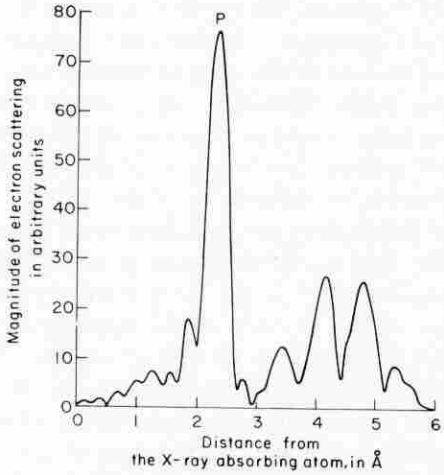

Fig. 6. The Fourier transform of $k\chi(k)$ for the data for copper of fig. 1. The major peaks correspond to the first few nearest neighbour atoms. The small wiggles are artefacts of the transform and the two small side peaks about the large first neighbour peak P are associated with that peak.

Another method employed to interpret EXAFS is to model the structure of the unknown and vary the model so as to have its calculated EXAFS best fit the measured values. In practice, except for the simplest cases, the number of parameters required to be varied is too great to make modelling a simple matter. The most useful way to employ modelling is in combination with Fourier transforming. The transform defines most of the parameters and modelling can be used to clarify a portion of the transform, such as the mixture of atoms in a given shell or separating two shells which are not resolved in the transform.

Besides the distance R_j, EXAFS contains other structure information as perusing eqn. (4) will indicate. The other structure information present are the number N_j and type of jth atoms in the shell at R_j and their mean square disorder σ^2 about the average distance R_j. All of this information can be obtained in favourable cases by a proper analysis of the EXAFS. Before illustrating this by discussing some applications of EXAFS we discuss how EXAFS is detected experimentally.

4. Detection of EXAFS

The detection of EXAFS requires monitoring some response which is proportional to the absorption of X-rays. The most straightforward method is to detect the absorption directly by monitoring the incoming I_0 and

transmitted I beams, simultaneously. From eqn. (1), μ is proportional to $\ln (I_0/I)$. For most applications absorption is the most precise and convenient method. However for some applications there are alternative monitoring methods which have advantages over the direct method.

4.1. *Dilute samples*

If the atoms whose EXAFS are to be measured are a very small fraction of the total number of atoms in the sample then the desired EXAFS is only a small part of the total absorption. In this case, isolating the desired EXAFS from the background of the rest of the sample requires subtracting two numbers, each much larger than their difference. Any small percentage error in the background introduces large errors in the desired EXAFS. To overcome this background problem it is desirable to use a monitoring technique which does not detect the background but detects only the signal. In principle, such a method is detection of the fluorescent radiation from the atoms excited by the absorbed X-rays. The fluorescent radiation is one mode of de-excitation of the excited atom. As illustrated in fig. 7 (a), fluorescence is the emission of a photon in the process of the excited atom relaxing to its ground state as electrons cascade down in energy to fill the core hole. For excitation of the K-shell, the most intense fluorescent radiation is the Kα radiation produced as a p-electron from the L-shell makes a transition to the K-shell hole. This radiation has a characteristic energy independent of and less than the exciting radiation energy. The number of atoms excited by the incoming radiation can be monitored by tuning to their fixed Kα fluorescent radiation energy. By doing this as a function of the energy of the incoming radiation one obtains data proportional to the absorption in the atoms of interest, the desired signal. The other atoms in the sample fluoresce at different energies, and, of course, the elastically scattered radiation is also at a different energy, and their contributions can be discriminated against by energy selection. Thus, in principle, the fluorescent signal has no background. In practice, the background is greatly decreased and it is possible to detect the EXAFS of atoms of greater dilution in fluorescence than is possible by absorption.

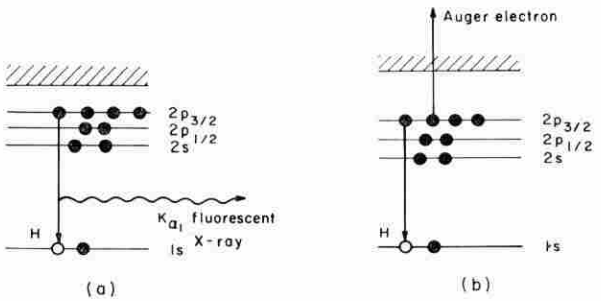

Fig. 7. Illustrating two possible modes of de-excitation of an excited atom with a hole in the 1 s shell (denoted by the unfilled circle). In (a) an electron in the $2p_{3/2}$ shell gives up its energy to a fluorescent X-ray as it makes its transition to the hole. In (b) the excess energy of the $2p_{3/2}$ electron as it drops to the 1 s hole is taken up by another $2p_{3/2}$ electron which is knocked free of the atom. This latter is an Auger electron.

4.2. *Surface enhancement*

Another mode of de-excitation of atoms is by Auger electron emission. In this process, illustrated in fig. 7 (*b*), as a bound electron of a fixed initial energy drops down to fill the core hole, it loses its energy by transferring it through the Coulomb interaction to another electron which is excited out of the atom. This excited electron can be detected and again has an energy characteristic of the atom from which it came. The same advantage of eliminating background occurs in detecting Auger electrons as for fluorescence. Yet, there is a significant difference between these two detection techniques. The fluorescent X-ray is about as penetrating as the incoming X-rays, and, thus, the signal comes from depths in the sample of the order of microns, typical penetration depths of X-rays. The Auger electron typically has a mean free path of the order of 1 nm = 10 Å. Therefore, in order to reach the detector, it must have originated from an atom quite near the surface.

This surface enhancement effect of Auger electrons can be put to advantage to study surface properties such as adsorbed surface layers. On the other hand, because only a small portion of the sample near the surface contributes, the signal is weak and difficult to detect. Detection of the Auger electrons requires a high vacuum environment limiting the application of this technique.

Both fluorescence and direct absorption detection can also be employed to study surface layers without the weakness of signal and high vacuum environment limitations of Auger electron detection. The surface enhancement can be gained by use of appropriate samples which have a large surface area to volume ratio as discussed in Section 6.1.

4.3. *Thick samples*

It is not always convenient to form samples in plane geometry thin enough for X-ray to transmit through. For such cases thick samples can be formed and the X-ray absorption monitored by detecting the fluorescence radiation. For the lighter elements the de-excitation process is dominated by Auger electron emission with little fluorescence. In this case the total photoelectron yield can be monitored without any attempt to discriminate for a particular electron such as the Auger one. One detects, then, a much larger signal consisting of not only the Auger electrons but the photoelectrons plus all of the secondary electrons created and able to escape the sample. The theoretical analysis of this detection process is obviously a mess and one cannot guarantee strict proportionality to X-ray absorption, though it is reasonable to hope that such is the case.

5. Comparison with other techniques

The characteristics of EXAFS give it certain advantages and disadvantages compared to the standard structure determining techniques. It is important to understand these in order to appreciate which systems can be advantageously studied by EXAFS.

All diffraction techniques directly detect long range order and, in particular, the unit of periodicity. To obtain information about the arrangement of atoms within the unit of periodicity, the unit cell, requires additional model making and calculations. For crystals with a large number of atoms in the

unit cell, such as biological proteins, the number of variables in a model are too great to solve by a calculation. This difficulty with diffraction methods occurs because only the intensity of the diffracted beam is detected and its phase information is lost. Several clever solutions to the phase problem have been developed which are used with spectacular success in mapping out the structure of crystallized forms of proteins.

For those forms of condensed matter which have no long range order, diffraction techniques have only limited applicability. A diffraction measurement on such aperiodic materials contains information on the sum of two particle correlation distances for all of the particles combined. When there are many different types of atoms present in the sample it is a hopeless case to separate out the contribution from each. In some special cases one can make the separation by use of neutron diffraction on various samples with the same chemical composition but with one isotope substituted for another. The scattering of neutrons from each isotope is generally different giving independent diffraction patterns for each isotopically different sample and permitting a separation into the contribution of each component.

The interaction of X-rays and neutrons with matter is usually weak enough for it to be possible to use the kinematic approximation to describe the diffraction process. The kinematic approximation assumes only one scattering of the incident beam by the atoms of the sample. The part of the beam scattered twice or more is assumed to be so weak in intensity as to be negligible. This kinematic approximation simplifies greatly the interpretation of diffraction data. In low energy electron diffraction (LEED) it is not possible to make this kinematic approximation. To determine more than the unit cell dimensions by LEED is a major computational undertaking, even in the simplest cases. When long range order ceases to exist, LEED is helpless.

The characteristics of EXAFS are complementary to those of diffraction techniques, so that it can be useful in many cases where they are inadequate. Thus, as EXAFS is sensitive only to *short range* order it can contribute to determining the arrangement of atoms within the unit cell. Aperiodic materials can be studied with the same ease as can crystals. The ability to determine the short range order about each type of atom, separately, by tuning X-ray energies to the absorption edge of interest is an advantage in the study of complicated materials composed of many different atoms. The ability to distinguish the type of nearest neighbour atoms by their backward scattering characteristics is advantageous. Finally, the direct relationship between the atomic structure in the vicinity of the absorbing atom and EXAFS makes its interpretation simple. We illustrate these characteristics by some examples in the next Section.

6. Applications

EXAFS is a relatively new technique. Its usefulness for structure determination was not clearly shown till 1971 (Sayers, Stern and Lytle 1971). It still remained a difficult experimental technique till the availability of synchrotron sources of X-rays in late spring of 1974. Almost all of the applications of EXAFS to structure determination have occurred since the latter date. It is safe to assume that its potential has not been fully explored and realized, as yet.

With this in mind we present here a representative sampling of structure determinations to date where EXAFS has played a significant role. In general, EXAFS is able to give useful information on only the first few neighbouring shells of atoms.

6.1. *Surface characterization*

EXAFS experiments on atoms adsorbed on surfaces provide a great deal of information about the location of the absorbed atoms relative to the substrate. It is possible to determine the distance between the adsorbed atoms and the substrate, whether the adsorbed atoms are mobile or attached above a given substrate site, and the location of this site. Such information can be obtained whether the adsorbed atoms are arranged periodically or not. Information about the vibrational motion of the adsorbed atoms and their location relative to other adsorbed atoms can also be obtained.

The system of molecular bromine Br_2 adsorbed on graphite has been studied. Graphite makes an interesting substrate. It consists of layers of carbon atoms arranged in a hexagonal array within the layers as illustrated in fig. 8. The binding within the layers, the basal planes, is strong while the binding between planes is by the relatively weak van der Waals force. Because of this anisotropic binding graphite is easily cleaved along the basal planes and small particles usually have a surface composed almost entirely of basal planes, and, thus, relatively homogeneous. To enhance the signal from adsorbed sub-monolayers (that is, incomplete ones) of Br_2, a form of graphite with a large surface area to volume ratio, called Grafoil, was used. Grafoil consists of small disc-shaped graphite particles which have been compressed and aligned so that for most of the particles the normals to the basal plane are parallel.

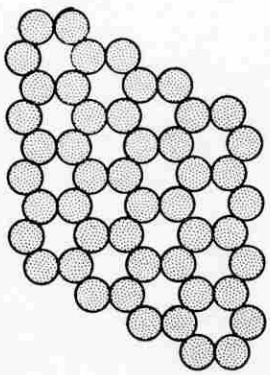

Fig. 8. The arrangement of the carbon atoms along part of the basal plane of graphite.

This macroscopic orientation of the graphite surfaces in Grafoil permits use of the anisotropy effect of EXAFS to determine the alignment of the molecular axis of any bromine atoms that remain molecular. The measurements are made with the X-ray polarization both parallel and perpendicular to the basal planes. Those molecules whose axes are *parallel* to the polarization give a maximum contribution to the K-edge EXAFS of Br while those molecules whose axes are *perpendicular* give zero contribution. Such a behaviour follows

from the dipole selection rule matrix element of eqn. (3). The p-state photoelectron that is excited from the initial s-state in the K-shell has an angular dependence of $\cos\theta$ where θ is the angle from the polarization direction. It is obvious that a scatterer at a point where the photoelectron has zero amplitude will not scatter the photoelectron, as is the case for Br–Br scattering in a molecule whose axis makes a $\theta = 90°$ angle with the polarization direction. A quantum mechanical calculation shows that the contribution of a scatterer at θ_i to the EXAFS varies as $\cos^2\theta_i$.

Three different coverages of Br_2 adsorbed on Grafoil were studied, namely, 0·2, 0·6 and 0·9 monolayers. A monolayer coverage corresponds to about 2×10^{-19} m$^2 = 20$ Å^2 area per Br_2, enough to permit the molecules to lie flat on the surface. The EXAFS at the K-edge of Br was studied. Two possible contributions to the EXAFS can be expected, backscattering from C and Br atoms. These are clearly distinguishable as seen from fig. 9 which shows the EXAFS for 0·2 monolayers of Br_2 adsorbed on Grafoil at room temperature (Stern *et al.* 1977). Because of their quite different k-dependence it is possible to separate out the contributions of Br–C and Br–Br scattering as indicated roughly in the figure. Analysis of the 0·2 monolayer data indicates a slight polarization dependence for the Br–C scattering but none discernable for the Br–Br scattering. Analysis of the Br–Br scattering shows that Br_2 remains molecular on being adsorbed, but the lack of any dependence on polarization shows that the molecular axis is not aligned relative to the surface. The presence of Br–C EXAFS of a single period indicates that the Br atom spends most of its time at a fixed distance relative to the C substrate and is not freely mobile on the surface.

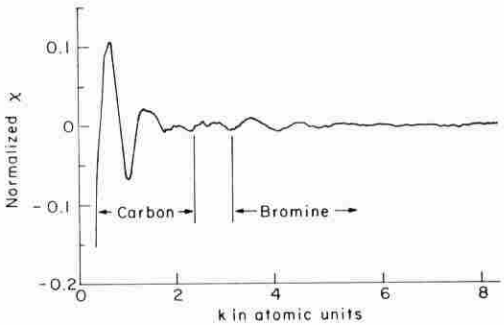

Fig. 9. The EXAFS of the K-edge of bromine when 0·2 monolayer of molecular Br_2 is adsorbed on the basal plane of graphite. The contributions from the surrounding carbon and bromine atoms are clearly distinguishable by their quite different variation with k, in agreement with the calculations of fig. 4.

The model that emerges from a more detailed study of the data is shown schematically in fig. 10. Its quantitative details are as follows. One end of the Br_2 molecule is fixed above the hexagonal site at $(2{\cdot}4 \pm 0{\cdot}1)$ Å from the nearest carbon atoms; and the Br–C bond makes an angle of $(42 \pm 3)°$ with the normal to the plane. The axis of the molecule pivots randomly about the fixed atom. The average Br–Br bond length in the adsorbed molecule is $(2{\cdot}25 \pm 0{\cdot}03)$ Å with parallel polarization. These are to be compared with the gaseous molecule distance of 2·283 Å. The Debye-Waller factor indicates

that the atoms in the molecule have a larger amplitude of motion relative to one another when adsorbed than they do in the vapour. The square of the amplitudes of the relative motion increases by 0·0025 Å^2 and 0·0053 Å^2 for polarizations normal and parallel to the graphite basal plane respectively, with an uncertainty of 0·0015 Å^2.

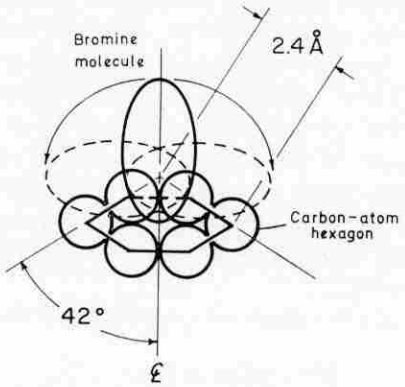

Fig. 10. A schematic representation of molecular bromine adsorbed in graphite at 0·2 monolayer coverage. A bromine molecule is pictured as an ellipsoid sitting on the carbon-atom hexagon. One atom of the bromine molecule is fixed above the hexagon site of the basal plane while the other end of the molecule is free to pivot about this atom. The Br–C bond is 2·4 Å in length making 42° with the normal.

For 0·6 and 0·9 monolayers a significant change occurs in the adsorbed Br_2 (Heald and Stern 1978). The molecules become aligned parallel to the surface and the Br–C distance increases to 2·9 Å. The alignment parallel to the surface is essentially complete at liquid nitrogen temperature but somewhat disordered at room temperature. The Br–Br distance increases about 0·03 Å above the vapour value of 2·283 Å. Each atom in the molecule is aligned as well as it can above adjacent hexagonal sites which are 2·46 Å apart. These results show that Br_2–Br_2 interactions which appear at the higher coverage are important in understanding the adsorbed layer configurations, and indicating that a simple picture of adsorption neglecting interactions between the adsorbed molecules is inadequate.

6.2. *Biological applications*

Metalloproteins are proteins whose molecules have only a few metal atoms among the hundreds of light atoms, such as carbon, nitrogen, oxygen and hydrogen, usually present. The metal atoms, which usually have a vital role in the function of the metalloprotein, can have their immediate environment investigated by EXAFS. Because there is no requirement of crystallinity in the use of EXAFS, the protein can be studied in solution under various chemical conditions to probe the structural changes around the metal atoms that occur during reactions. The main experimental limitation is how dilute the metal atoms can be allowed to become before their signal becomes too weak. With fluorescence detection techniques a few atomic parts per million seems to be the present limit.

The iron-sulphur protein rubredoxin, which has one iron atom, is the protein whose structure has been determined to the greatest accuracy of any by X-ray

diffraction; this first accurate analysis had indicated an anomalously shortened bond between one of the four sulphurs adjacent to the iron atom. But EXAFS studies showed no such anomalously shortened bond (Shulman *et al.* 1975; Sayers *et al.* 1976) and this was subsequently verified by new X-ray diffraction results.

The protein haemerythrin with two irons which serves the analogous function in some marine animals as haemoglobin does for humans, namely, oxygen transport and transfer, has had its structure determined by two different X-ray diffraction groups. These structure determinations were performed on haemerythrin from different marine animals, one from the west coast and the other from the east coast of the United States, and claimed different atomic arrangement around the irons in each case. EXAFS studies of samples of haemerythrin from the same two marine animals showed that the two samples had exactly the same atomic environment and showed which diffraction determination was correct.

The enzyme carbonic anhydrase which catalyzes the reaction

$$H^+ + HCO_3 \rightleftharpoons H_2O + CO_2$$

has a zinc atom at its active site. X-ray diffraction studies of the protein human carbonic anhydrase C at 2·5 Å resolution had indicated that iodine ions bonded at 3·5–3·7 Å from the zinc atom which implies that they do not bind directly to the zinc. An EXAFS study of bovine carbonic anhydrase B by Brown, Navon and Shulman (1977) showed that the iodine ions bind directly to the zinc atom at a distance of $2{\cdot}65 \pm 0{\cdot}06$ Å. Unless there is an unexpected difference between these two forms of the enzyme it appears that the X-ray data either mislocated the iodine ion or there is another binding site further from the zinc site.

6.3. *Liquids, glasses and amorphous solids*

Complex aperiodic forms of condensed matter such as liquids, glasses, and amorphous solids consisting of more than one component can advantageously be studied by EXAFS. Since the atoms in such materials have no periodic arrangement, a complete definition of the structure would have to define the location of every one of the order of 10^{23} atoms in the material as a function of time. Clearly such a description would be impossible to assimilate even if it could be ascertained, which of course it cannot. One practical way to describe an aperiodic sample is in terms of all of the partial two-particle correlation functions $P_{AB}(r)$ which give the probability of finding a type A atom a distance r from an origin which contains a type B atom. Standard diffraction techniques determine the superposition of all such two-particle correlation functions,

$$P(r) = \sum_A \sum_B P_{AB}(r).$$

EXAFS can straightforwardly determine

$$\sum_A P_{AB}(r),$$

and in favourable cases, can determine $P_{AB}(r)$ itself.

The glass GeO_2 was studied with EXAFS by Sayers *et al.* (1975). Comparing its EXAFS with that of the crystalline α-quartz form it was possible to obtain a more precise measure of the structural disorder in the glass than was available from diffraction measurements. The germanium atom in crystalline GeO_2 is surrounded by four oxygen atoms in a tetrahedral arrangement. Each tetrahedron is connected to four others by sharing a single common oxygen atom at the corners. The EXAFS measurements showed that in the glass the GeO_4 tetrahedron (fig. 11) is rigid within experimental accuracy. The long-range disorder in the glass is introduced by the manner in which the tetrahedra are connected to one another. The angle between Ge–O–Ge atoms (fig. 11) is no longer precisely 130°, but with a $\pm 6{\cdot}5°$ r.m.s. deviation.

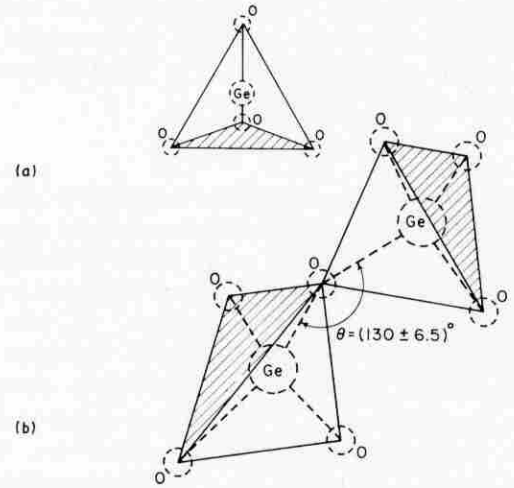

Fig. 11. The structure of GeO_2 glass as determined by EXAFS. The tetrahedron, consisting of a central Ge atom with O atoms in the corners, is found to be a rigid unit. The GeO_4 tetrahedron is as illustrated in (*a*). Each of its sides is an equilateral triangle. The glass is formed of tetrahedra attached to one another by sharing a single oxygen at each corner. The long-range order is destroyed when there is a r.m.s. deviation of 6·5° in the angle between Ge–O–Ge from the value of 130° found in the 'α-quartz' crystalline form, as illustrated in (*b*).

Both the amorphous and liquid states of As_2Se_3 have been studied by EXAFS in the temperature range 100 K–773 K by Crozier *et al.* (1977). Just as in GeO_2 the nearest neighbours in the amorphous form are similar to the crystalline form. There is not a major structural rearrangement in the nearest neighbour shell when amorphous As_2Se_3 melts. However, the data suggest that small structural changes may occur at the melting point, namely, a slight increase in the nearest neighbour As–Se distance, a slight decrease in the number of nearest neighbours, and perhaps a slight decrease in the r.m.s. disorder of the nearest neighbour distance.

6.4. *High pressure studies*

The techniques available today for exerting static high pressures on samples in the hundreds of kilobars range employ small samples surrounded by relatively massive anvils. This limits the angular range available to measure

scattered or diffracted radiation, but, even more severe a problem, when phase transformations occur at such high pressures the sample, even if it were originally a single crystal, ends up in a polycrystalline form whose preferred orientations are unknown. With such a sample it is not possible to obtain, by diffraction, any more reliable information about crystal structure than the shape of the unit cell. EXAFS can supplement diffraction results with information about the location of atoms *within* the unit cell.

EXAFS measurements have been made on pyrite FeS_2 (iron pyrites) in such an apparatus up to pressures of 64 kbar by Ingalls *et al.* (1978). The Fe–Fe distance in pyrite corresponds to one dimension of the unit cell and its variation with pressure agrees with high pressure X-ray diffraction measurements. In contrast, EXAFS showed that the Fe–S spacing in pyrite is considerably less compressible. The determination of both the Fe–Fe and Fe–S spacing completely defines the positions of the atoms within the pyrite unit cell throughout this pressure range. The EXAFS measurements should be extendable up to hundreds of kilobars.

6.5. *Catalysts*

Catalysts are substances that accelerate chemical reactions without being used up themselves. Catalysts are of great commercial importance, playing a major role in producing goods worth more than $100 billion a year. The chemical industry, for example, is dependent on catalysts for converting crude oil into useful products such as petrol and plastics. In spite of the importance of catalysts, our knowledge of their basic mode of operation is so limited as to have almost no predictive value. One difficulty in analysing catalysts is that their forms as used commercially are not well characterized since they are contaminated with undetermined amounts of impurities, many of which are in a highly dispersed form. In short, there is a large gap between commercial catalysts and the ideal samples studied in the laboratory. Here, EXAFS has the advantage of enabling one to study real catalysts under actual operating conditions and still have hope of observing what is occurring at the atomic level.

The interaction of a highly dispersed ruthenium-silica catalyst with oxygen was studied with EXAFS by Lytle, Via and Sinfelt (1977). This catalyst consists of ruthenium metal particles so small that surface atoms constitute a large fraction of the total number of atoms present. The small metal particles are dispersed on a large-area silica substrate whose configuration is inherently not well characterized. The initially reduced catalyst was exposed to oxygen at 25°C and 400°C. Because of their different k-dependence backscattering functions, ruthenium and oxygen alone are easily distinguished from one another in the EXAFS spectra. In the reduced form no oxygen was found present, each ruthenium atom was surrounded by about 8 other ruthenium atoms, substantially less than the 12 found for the atoms of ruthenium as bulk material. This result is consistent with electron microscopy studies in conjunction with gas adsorption data which suggest that the catalyst consists of ruthenium clusters present largely in the form of raft-like structures comprising single layers of atoms.

When the catalyst is exposed to oxygen at 25°C the EXAFS analysis finds that the oxygen is adsorbed on the surface and does not produce a bulk oxide. However, bulk oxidation does occur at 400°C. Futher analysis of the data

leads the authors to conclude that the oxygen O_2 molecules are adsorbed as molecules in an ' end-on ' configuration, analogous to the Br_2 adsorption on graphite at low coverage, at positions which have threefold symmetry in relation to the ruthenium surface atoms.

7. Sources

The direct measurement of X-ray absorption is, in principle, very simple (see fig. 2, page 291). Complications enter because data must be taken at a large number of points, and high intensity sources of continuous X-radiation are rather large installations. Standard sources of X-rays consist of an anode placed at a high positive voltage relative to a heated filament which acts as a source of electrons. The electrons are accelerated to the anode and in the process of colliding with the atoms of the anode they give up their energies, in part, in producing X-rays. The deceleration of the electrons in the electric fields near the nuclei of atoms produces a continuum of X-radiation up to a maximum photon energy $\hbar\omega$ equal to the kinetic energy of the electrons. In addition, discrete lines of X-radiation characteristic of the atoms in the anode are produced by excited atoms emitting fluorescent radiation as they make transitions from one discrete state to another. The intensity in the characteristic radiation is of the same order as the integrated intensity of the continuum radiation. For EXAFS measurements it is the continuum radiation that is required. The intensity from a typical EXAFS setup using conventional sources is about 10^3–10^4 X-ray photons per second (Lytle *et al.* 1975). A total of about 10^6 counts per point is required to attain the minimum acceptable statistical accuracy of about one part in a thousand for EXAFS measurements. A typical time to accumulate data of such minimum accuracy using conventional X-ray tube sources is about a week. However, there are many measurements that require accuracy greater by even an order of magnitude than this.

Fortunately, for EXAFS experiments, a new and much more intense source of continuum X-radiation became available in 1974 utilizing the synchrotron radiation emitted from the electron–positron storage ring at Stanford, California. This source is about 10^4 times more intense in the X-ray continuum than a standard source, and has made practical the development of computer-controlled facilities which can make a routine measurement of an EXAFS spectrum in 20 min, and has also made feasible the measurements of specimens containing only dilute amounts of the atoms that are of interest. Other EXAFS facilities utilizing synchrotron radiation sources are now becoming available or are planned to be built in the near future.

This article has explained the characteristics of EXAFS and has presented a few representatives of its applications. It has not attempted to give a full review, but rather to indicate the new avenues in structure determination which it is opening.

Acknowledgment

I wish to thank Prof. I. Steinberger and the Racah Institute of Physics of the Hebrew University of Jerusalem for their hospitality during the time this manuscript was written.

References

Azaroff, L. V., and Pease, D. M., 1974, Chap. 6 in *X-ray Spectroscopy* (McGraw-Hill Book Co., 1974, N.Y., N.Y.), ed. L. V. Azaroff.

Brown, G. S., Navon, G., and Shulman, R. G., 1977, *Proc. Natl. Acad. Sci. U.S.A.*, **74,** 1794.

Crozier, E. D., Lytle, F. W., Sayers, D. E., and Stern, E. A., 1977, *Can. J. Chem.*, **55,** 1968

Heald, S., Stern, E. A. 1978, *Phys. Rev.* B, **17,** May 15

Ingalls, R., Garcia, G. A., and Stern, E. A., 1978, *Phys. Rev. Lett.*, **40,** 333.

Lee, P. A., and Beni, G., 1977, *Phys. Rev.* B, **15,** 2862.

Lytle, F. W., Sayers, D. E., and Stern, E. A., 1975, *Phys. Rev.* B, **11,** 4836.

Lytle, F. W., Via, G. H., and Sinfelt, J. H., 1977, *J. Chem. Phys.*, **67,** 3831.

Sayers, D. E., Stern, E. A., and Lytle, F. W., 1971, *Phys. Rev. Lett.*, **27,** 1204.

Sayers, D. E., Stern, E. A., and Lytle, F. W., 1975, *Phys. Rev. Lett.*, **35,** 584.

Sayers, D. E., Stern, E. A., and Herriott, J., 1976, *J. Chem. Phys.*, **64,** 427.

Shulman, R. G., Eisenberger, P., Blumberg, W. E., and Stambaugh, N. A., 1975, *Proc. Natl. Acad. Sci. U.S.A.*, **72,** 4003.

Stern, E. A., 1974, *Phys. Rev.* B, **10,** 3027.

Stern, E. A., Sayers, D. E., Lytle, F. W., 1975, *Phys. Rev.* B, **11,** 4836.

Stern, E. A., Sayers, D. E., Dash, J. G., Shechter, H., and Bunker, B., 1977, *Phys. Rev. Lett.*, **38,** 767.

The Author:

Edward A. Stern is Professor of Physics in the University of Washington at Seattle, a post he has held since 1965. He graduated Ph.D. at California Institute of Technology in 1955, and was a Post-Doctoral Fellow there from 1955 to 1957. From 1957 to 1965 he was successively Assistant Professor and Associate Professor at the University of Maryland.